

UNCLASSIFIED

Defense Technical Information Center  
Compilation Part Notice

ADP011775

TITLE: A One-Dimensional Photonic Bandgap System as  
High-Reflectivity Mirror for Microwave and THz Applications

DISTRIBUTION: Approved for public release, distribution unlimited

This paper is part of the following report:

TITLE: International Conference on Terahertz Electronics [8th], Held in  
Darmstadt, Germany on 28-29 September 2000

To order the complete compilation report, use: ADA398789

The component part is provided here to allow users access to individually authored sections of proceedings, annals, symposia, etc. However, the component should be considered within the context of the overall compilation report and not as a stand-alone technical report.

The following component part numbers comprise the compilation report:

ADP011730 thru ADP011799

UNCLASSIFIED

# A One-Dimensional Photonic Bandgap System as High-Reflectivity Mirror for Microwave and THz Applications

Gerhard W. Schwaab

**Abstract** – A one-dimensional photonic bandgap mirror (PBM) has been designed consisting of periodically alternating planar quarter-wavelength layers of a high-refractive index dielectric and low-refractive index material (e.g. vacuum). A V-shaped folded Fabry-Perot-Interferometer was set up with two scaled PBMs and a spherical metal mirror to provide a stable resonator design. The PBMs consisted of polystyrene and air as dielectrics and were designed for a center frequency of 23.44 GHz. The transmission characteristics of the FPI was measured for different numbers of layers in the PBMs. The reflectivity of the PBMs was derived from the cavity's chromatic resolving power. The measured reflectivity and bandwidth are compared with theoretical expectations taking into account resonator losses and absorption in the dielectrics.

## I. INTRODUCTION

The THz spectral range is especially important for spectroscopic applications since the lowest vibrational levels of large molecules (e.g. skeletal motions of biomolecules), the vibrational levels of small molecular clusters, and the energy states of molecules bound to a surface lie in that frequency region. Due to their low energies, THz photons are in general not able to break the bonds of weakly bound molecular systems. As radiation sources, several options are possible like BWOs (direct or multiplied), laser sidebands [1,2,3], optical mixers [4,5], or p-type Ge lasers [6]. The different sources strongly differ with respect to frequency range, output power, and spectral purity.

p-type Ge lasers provide the most promising aspects for an improved spectrometer for the frequency range between 1 and 4 THz, since they are solid state devices and they can easily be tuned by changing the magnetic field. p-type Ge lasers are characterized by their pulsed operation and a longitudinal mode spacing which is defined by the length of the laser crystal. To improve these systems, they have to be operated with an external resonator and anti-reflection coated front surfaces.

Pulsed lasers are even needed for cavity ringdown spectroscopy [7], where instead of directly measuring the absorption of a gas, the Q-factor of a resonator cavity is measured with and without an absorbing gas. Briefly, a high-Q resonator is illuminated by a short laser pulse. At the resonator output an exponentially decaying series of signal pulses appears whose decay time is a measure of the resonator quality. An absorbing gas in the resonator will change this decay time in a way that the absorption coefficient can be calculated.

Summarizing, to be able to develop a new type of TuFIR spectrometer, one major optical problem is the design of wideband high-reflectivity FIR mirrors.

## II. THEORETICAL BACKGROUND

Wideband mirrors with high reflectivity (>99.5%) are well known in the optical and IR regions, where they serve for example as laser mirrors. They consist of a substrate that is coated with a stack of quarter wavelength layers with alternating high ( $n_h$ ) and low ( $n_l$ ) indices of refraction. The quality of such a mirror is determined by the number of layers, the ratio  $n_{rel}=n_h/n_l$  and the absorption and diffraction losses within the different layers. The reflection and transmission of a multilayer optics can be calculated recursively by taking into account the reflections and transmissions at the boundaries between different layers and the phase delay within one layer. Weak dielectric absorption losses can be accounted for by using complex indices of refraction. Figure 1 shows a N-layer system with layer thickness  $d_i$ , index of refraction  $n_i$ , and propagation angle  $\theta_i$  for the i-th layer. With the incident electric field  $E_i$  and the reflected electric field  $E_r$ , the total field reflection coefficient  $\rho_j = \frac{E_r}{E_i}$  of layers j+1 through N can be calculated [8]. Within a real system additional losses occur. Most important are resonator losses and losses due

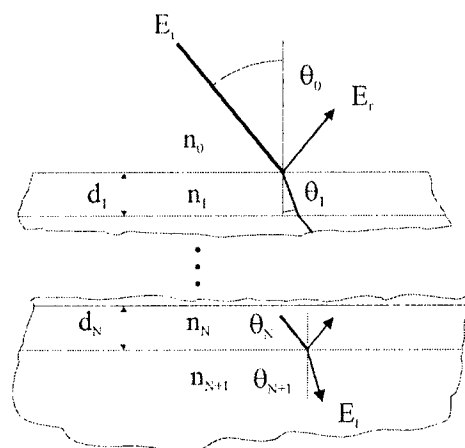


Fig. 1: Schematic of a N-layer optics with incident field  $E_i$ , reflected field  $E_r$ , and transmitted field  $E_t$ . Each layer is described by its thickness  $d$ , its refractive index  $n$ , and its propagation angle  $\theta$ .

G. W. Schwaab is with the Lehrstuhl für physikalische Chemie II, Ruhr-Universität Bochum, Universitätsstrasse 150, 44780 Bochum

to misalignment which show a different frequency behavior than the dielectric losses. They can be accounted for [9] by modifying the one way phase shift  $e^{i\delta_{j+1}}$  (with complex  $\delta_{j+1}$ ) to  $e^{-\tau} e^{i\delta_{j+1}}$  with the additional loss factor  $e^{-\tau}$ . This leads to an electric field reflection coefficient of:

$$\rho_j = \frac{r_{j,j+1} + \rho_{j+1} e^{-2\tau} e^{2i\delta_{j+1}}}{1 + r_{j,j+1} \rho_{j+1} e^{-2\tau} e^{2i\delta_{j+1}}} \quad (1)$$

Here,  $r_{j,j+1}$  represents the field reflection coefficient at the boundary of layers  $j$  and  $j+1$ , which is given by the Fresnel formulae [10]  $\rho_{j+1}$  the total field reflection coefficient of layers  $j+2$  through  $N$ ,  $i$  the  $\sqrt{-1}$ , and  $\delta_{j+1}$  the phase delay in layer  $j+1$ . The phase delay is given by the relationship

$$\delta_j = 2 \pi \frac{\nu}{c} n_j d_j \cos \theta_j \quad (2)$$

with  $c$  the velocity of light and  $\theta_j$  the propagation angle of the radiation in layer  $j$ . The  $\theta_j$  can be calculated from the incident angle  $\theta_i$  using Snellius' law.

The electric field transmission coefficient is given by

$$\tau_j = \frac{\frac{n_{j+1} \cos \theta_{j+1}}{n_j \cos \theta_j} t_{j,j+1} \tau_{j+1} e^{-\tau} e^{i\delta_{j+1}}}{1 + r_{j,j+1} \rho_{j+1} e^{-2\tau} e^{2i\delta_{j+1}}} \quad (3)$$

Here,  $t_{j,j+1}$  represents the Fresnel field transmission factor at the boundary between layers  $j$  and  $j+1$  as calculated by traversing from layer  $j$  into layer  $j+1$ . Please note, that for the transmission formula the layers are counted just opposite to the labeling in Figure 1 so that the numbers increase looking backward from the transmitted beam.

The power reflection and power transmission coefficients can be calculated from  $\rho_j$  and  $\tau_j$  by taking the absolute square value, respectively. The phase shift is given by the overall argument of the expression.

To be able to theoretically study these problems, a Mathematica program has been developed, that includes iterative handling of multilayer optical problems and second order effective media theory to simulate artificial dielectrics.

### III. WIDEBAND DIELECTRIC MIRRORS FOR HIGH-Q THZ RESONATORS

Since a quarter wavelength in the mm-wave to THz spectral regions is in the order of a few to a few hundred micrometers, such layers can currently not efficiently be fabricated by epitaxial or etching techniques. It is, however, possible to fabricate lambda quarter dielectric sheets from different materials ranging from polyethylene to silicon. The simplest possible way to build a high-reflectivity mirror is therefore to stack alternating  $\lambda/4$ -layers of materials with high and low index of refraction (see Fig. 2, top).

Using air as the low index of refraction dielectric, best results are expected for low-loss dielectrics with a high index of refraction like high-purity Si ( $n=3.42$ ), which

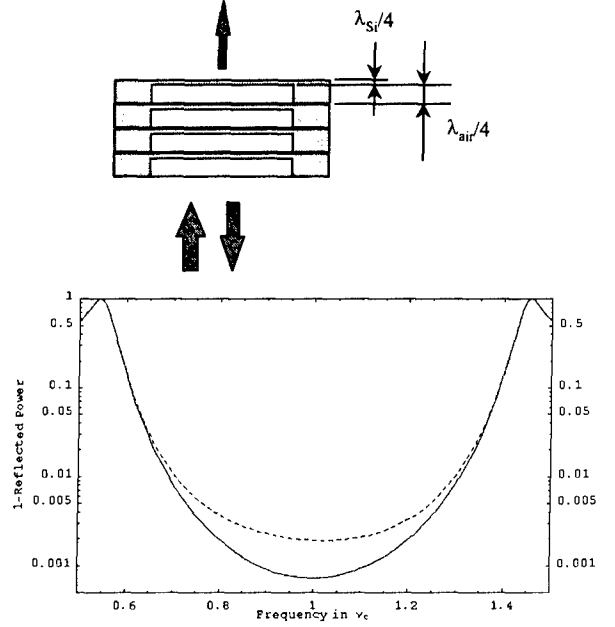


Fig. 2: top: Stack of four  $\lambda/4$  doublets in air and Si as high-reflectivity THz mirror. bottom: 1-Reflectivity versus relative frequency for lossless Si (solid line) and Si with a loss tangent of 0.0012 (dashed).

shows low absorption in the design frequency range from 1-4 THz and can be grind down to a layer thickness of less than 7  $\mu\text{m}$ .

Calculations were performed for four  $\lambda/4$ -layers of Si separated by  $\lambda/4$ -layers of air. Fig. 2, top, shows 1- $\rho$  of such a system,  $\rho$  being the power reflection coefficient. For lossless material, reflectivities higher than 99.9 percent can be achieved with a relative bandwidth of more than 20%. Introducing a loss tangent of  $12 \times 10^{-4}$  as it has been described in the literature [11] leads to a reduced reflectivity of 99.8% maximum and a bandwidth of about 50% for reflectivities higher than 99.5%.

### IV. A SCALED MICROWAVE DEMONSTRATOR

Due to the high cost of the ultrathin Si slices described above, a 100:1 scaled mirror model was built. It consisted of up to 10 layers of polystyrene sheets with a thickness of  $d=2$  mm and a length of 300 mm square. To prevent bending of the sheets and to keep the layer spacing constant over the full mirror area four  $5 \times 5 \text{ mm}^2$  evenly distributed cork spacers were glued to each sheet. The index of refraction of polystyrene is  $n=1.6$ . This corresponds to a design wavelength of  $\lambda = 4 n d = 12.8$  mm or a design frequency of  $\nu = c/\lambda = 23.4$  GHz. The size of the air gap between two adjacent polystyrene sheets was therefore chosen to be 3.2 mm. Literature values for the loss tangent of polystyrene [12] are in the order of  $\tan \delta = 1 \times 10^{-4}$  to  $1.2 \times 10^{-3}$ . Expected reflectivities range from 99.97% (lossless material) to 99.5% ( $\tan \delta = 1.2 \times 10^{-3}$ ).

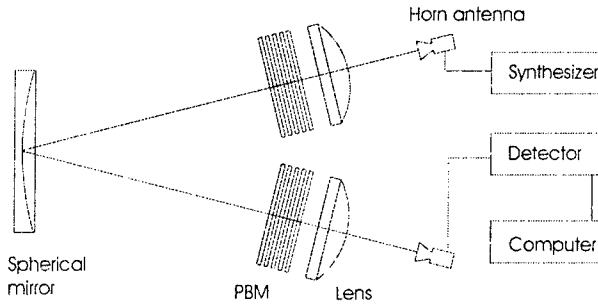


Fig. 3 V-shaped folded Fabry-Perot set-up to determine the reflectivity of the photonic bandgap mirrors.

To measure the mirror reflectivity, a folded confocal Fabry-Perot-interferometer (FPI) was designed (see Figure 3) with two PBMs as input and output ports and a single spherical aluminum mirror with a radius of curvature of 2400 mm and a diameter of 410 mm to re-focus the beam. The length of the FPI was adjustable and was fixed at 2.4 m. The angle between the two arms of the interferometer was  $7^\circ$ . The electric field distribution inside the interferometer can be described by Gaussian resonator modes, the  $TEM_{00}$  mode being the strongest one (see Figure 5, right). The folding of the resonator leads to an astigmatism which results in slightly different beam waists for the beams parallel and perpendicular to the interferometer plane.

One arm of the FPI was irradiated by microwave radiation from a HP83640B synthesizer. A crystal detector was used to detect the transmitted output power. The data taking process was fully computerized. Two wideband rectangular horn antennas transformed the microwave radiation to free space. Plano-convex HDPE lenses with a diameter of 260 mm and a focal length of  $f=480$  mm were used to match the interferometer input and output beams to the horn antennas.

Given the measured transmitted power  $P_m$  and the incident power  $P_0$  and assuming identical mirrors at input and output of the interferometer, the frequency dependency  $T[v]$  of the relative transmitted power  $T=P_m/P_0$  around a transmission maximum is given by

$$T[v] = T_0 \frac{1}{1 + \frac{4\rho}{(1-\rho)^2} \sin^2\left[\frac{2\pi(v-v_0)}{2\Delta v}\right]} \quad (4)$$

Here,  $T_0$  represents the maximum transmitted relative power,  $\rho$  the power reflectivity of a single mirror,  $v_0$  the center frequency of the transmission maximum, and  $\Delta v=c/2L$  the free spectral range of the interferometer.

The transmission spectrum of the interferometer was recorded from 20 to 26 GHz as a function of the number of dielectric layers (1 to 10 layers per mirror). The spectral resolution was chosen according to the expected transmission line width ranging from 1 MHz for a small number of layers to 0.05 MHz for a large number of layers.

The recorded power spectrum was linearized using calibration data for the power detector. Each  $TEM_{00}$  transmission peak was fitted using a non-linear least square fit. To minimize cross-talk effects from higher

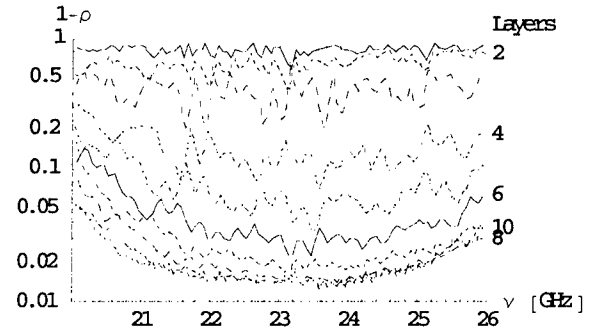


Fig. 4 Measured  $1-\rho$  as function of the number of polyethylene layers per mirror versus frequency.

order Gaussian modes, only the frequency range close to the center frequency was used in the fit with the highest frequency coverage for small number of layers and a smaller frequency range for a large number of layers. The model was validated by using a theoretical transmission spectrum and by analysing it the same way than the measured spectra. The results obtained were compared with directly calculated power reflection coefficients and showed excellent agreement.

Figure 6 shows in logarithmic scale  $1-\rho$ , the measured power reflection coefficient, as a function of the number of dielectric layers. As expected, for  $N_L=1$  to 7 the power reflection increases with increasing  $N_L$ . However, increasing  $N_L$  from 8 to 10, only little improvement in  $\rho$  can be observed. The maximum reflectivity obtained by this method was  $\rho = 98.7\%$

## V. DISCUSSION

The maximum achieved power reflectivity is considerably less than what is expected from theory, even taking loss factors as large as  $\tan\delta=0.0012$  into account. This discrepancy between theory and experiment is at least partly due to resonator losses. A good measure to discuss resonator losses is the Fresnel number  $N_f = a^2/(L\lambda)$  with  $2a$  being the diameter of the resonator end mirrors,  $L$  the resonator length, and  $\lambda$  the wavelength of the radiation. An approximate formula for the resonator loss of a confocal resonator with circular end mirrors is given by [9]

$$\delta \approx 16\pi^2 N_f \exp(-4\pi N_f) \quad \text{for } N_f \geq 1. \quad (5)$$

That for a confocal resonator with square mirrors is given by

$$\delta \approx 8\pi\sqrt{2N_f} \exp(-4\pi N_f) \quad \text{for } N_f \geq 0.5 \quad (6)$$

Although the resonator described here has planar end faces, due to the re-focusing mirror, the formulae for confocal mirrors apply. The definition of the relevant size  $a$  is ambiguous, however, because it is unclear, if the size of the spherical mirror or the size of the PBMs is the relevant dimension. Since the lateral dimensions of the PBMs leads to a smaller  $N_f$  and therefore larger resonator losses, we used the second formula to compare theoretical transmission spectra with the experimental results.

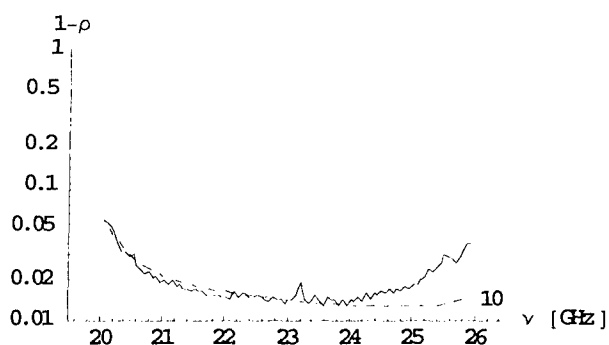


Fig. 5  $1-\rho$  as function of frequency for a photonic bandgap mirror with 10 polystyrene-air-layers (solid). The dashed curve shows theoretical values obtained assuming  $N_f=0.833$  and an additional frequency independent loss of 0.4% per pass.

From this comparison, it is evident, that the critical dimension  $a$  is larger than 0.155 m. With a resonator length  $L=2.4$  m and  $\lambda=12.8$  mm, the Fresnel number for the folded Fabry-Perot interferometer is larger than 0.8 at band center.  $N_f$  and therefore  $\delta$  are strongly frequency dependent leading to large losses at low frequencies, if  $a$  is underestimated. Thus taking only resonator losses into account cannot resolve the described discrepancy.

The theoretical data agree better with the experimental results, if an additional frequency independent loss of 0.4% per pass is included. But even then, the agreement is not perfect at the high frequency end of the reflectivity curve (see figure 6).

There are several mechanisms, that might be responsible for such a high frequency effect. The most important ones are the surface roughness of the metal mirror, deviations of the metal mirror surface from the ideal spherical shape, and spacing and shape deviations in the photonic bandgap mirrors. Currently, investigations are under way, which of these effects plays the most crucial role.

Recursive multilayer optics can be used to design high-reflectivity mirrors for advanced TuFIR spectrometers. The demonstration of the feasibility of high reflectivity FIR mirrors facilitates the design of new FIR resonators as they are needed for FIR cavity ringdown spectroscopy or for external resonators of p-type Ge lasers.

The next steps towards an advanced TuFIR spectrometer are the experimental clarification of the additional losses found in the scaled microwave model and the setup of a higher frequency system which can be used for spectroscopy. Eventually, the extension of the frequency and power range accessible to TuFIR spectroscopy will lead to an improved understanding of molecular systems as they can be found on earth and in space.

#### Acknowledgement

It is a pleasure to acknowledge the support of Dirk Plettemeier from the Institute of High Frequency Techniques at the Ruhr-Universität Bochum who supplied the wide-band horn antennas and the programming skills of Holger Krumm who considerably facilitated the measurement procedure.

#### References

1. D.D. Bicanic, B.F.J. Zuidberg, A. Dymanus, *Appl. Phys. Lett.* 32, 367 (1978).
2. P. Verhoeve, E. Zwart, M. Drabbels, J.J. ter Meulen, W. L. Meerts, A. Dymanus, D. B. McLay, *Rev. Sci. Instrum.* 61, 1612 (1990)
3. G.A. Blake, K.B. Laughlin, R.C. Cohen, K.L. Busarow, D.H. Gwo, C.A. Schmittenmaer, D.W. Steyert, R.J. Saykally, *Rev. Sci. Instrum.* 62, 1701 (1991)
4. S. Matsuura, G.A. Blake, R.A. Wyss, J.C. Pearson, C. Kadow, A.W. Jackson, A.C. Gossard, *Traveling-Wave Photomixers Based on Noncollinear Optical/Terahertz Phase-Matching*, Proceedings of the 10<sup>th</sup> International Symposium on Space Terahertz Technology, Charlottesville, Virginia, 1999.
5. E. Duerr, K. McIntosh, S. Verghese, „Design of a Distributed Photomixer for Use as Terahertz Local Oscillator, . Proceedings of the 10<sup>th</sup> International Symposium on Space Terahertz Technology, Charlottesville, Virginia, 1999
6. E. Bründermann, D.R. Chamberlain, E.E. Haller, „Novel Design of Widely Tunable Germanium Terahertz Lasers“, *IR Phys. & Techn.* 40, 141-151 (1999)
7. J.J. Scherer, D. Voelkel, D.J. Rakestraw, J.B. Paul, C.P. Collier, R.J. Saykally, A.O. Keefe, *Chem. Phys. Lett* 245, 273-280 (1995)
8. D.H. Raguin, G.M. Morris, *Appl. Optics* 32, 1154 (1993)
9. A.E. Siegman, „Lasers“, Chapter 19, University Science Books, Mill Valley, California
10. Bergmann-Schaefer, *Lehrbuch der Experimentalphysik Band III, Optik*, 7<sup>th</sup> Edition, p. 452, Walter de Gruyter, Berlin 1978,
11. P.F. Goldsmith, „Quasioptical Systems“, Chapter 5.4, IEEE press, New York, 1998
12. A.J.Bur, “Dielectric properties of polymers at microwave frequencies: a review”, *Polymer* 26, 963-977, (1985)